Colloid and Interface Science Communications 42 (2021) 100416

Contents lists available at ScienceDirect

Colloid and Interface Science Communications

journal homepage: www.elsevier.com/locate/colcom

# Development of new adsorbents via microwave treatment magnetic PET synthesis from waste PET and investigation of TC removal

Mehtap Ersan *, Hatice Dogan

*Cumhuriyet University, Faculty of Engineering, Chemical Engineering Department, 58140 Sivas, Turkey*

ARTICLE INFO

*Keywords:*
Adsorption
Waste pet
Microwave energy
nZVI
Tetracycline

ABSTRACT

In this study; new, economic and environment friendly adsorbents were synthesized using waste polyethylene terephthalate based adsorbent, derived from waste PET bottles, WPET, nano-scale zero valent iron modified adsorbent nZVI-WPET and microwave energy pre-treatment applied adsorbent MW/WPET-nZVI for TC removal. The synthesized composite was characterized using various techniques such as EDX, FT-IR XRD and SEM. Maximum adsorption values were obtained for all adsorbents at pH 5.0, with adsorbent amount of 10.0 g/l, at 20 C' and with initial TC concentration of 50 mg/l as a result of which the highest adsorption yield was obtained for WPET, WPET- nZVI and 2 min MW/WPET- nZVI as; 92.42%, 93.10%, 93.38% respectively. Maximum adsorption capacities, values were determined as 67.11 mg/g, 80 mg/g and 105.26 for WPET, WPET-nZVI and 2 min MW/WPET-nZVI. Adsorption isotherms parameters were modeled for new adsorbents and the best fit achieved with Freundlich isotherms for TC removal process.

## 1. Introduction

Polyethylene teraphytalate (PET) is among the most frequent industrial packing material. PET is thermoplastic polyester, it is a type of plastic and is widely used in pharmaceutics, food and beverage cups since it is economic, strong, transparent and easily shaped and thus its wastes emerge as a significant problem resulting in environmental pollution worldwide [1]. On average 4.8–12.7 million metric tons of plastic waste reach the oceans on an annual basis and approximately 1.7–4.4% of this waste comes from coastal countries [2]. European Commission reported that PET waste amounts to more than 8% by weight of the total solid waste in the World which is a signficiant threat for environmental health [3]. Moreover, since the degradation of waste PET requires 180 years, recycling is the only solution to reduce environmental pollution [4]. which makes it mandotory to eliminate PET waste. Energy recovery, chemical recycling, feedstock recycling and carbon based materials as actived carbon production can be cited as examples of various elimination processes [5]. Active carbon materials syhenthesized two ways. (i) the physical technique consists of carbonization of the precursor in an inert atmosphere followed by gasification and high porosity carbons can be obtained of char burn-off (ii) the chemical technique is based upon the modification of the surface chemistry of active carbon through chemical activation processes. Active carbon is used as an adsorbent due to its high specific surface area, well-developed internal pore structure, good chemical and thermal stability, good mechanical strength and several surface functional groups. Active carbon is characterized by its low density, easy regeneration and suitability for large scale production, which can be modified chemically in the presence of a specific solvent [4–6]. It is known as a highly effective adsorbent for polluted solutions due to its appropriate physical and chemical characteristics. Pet waste is a good source of activated carbon for 'Green Synthesis' applications but does not have the functional groups to which metal ions or organic molecules in the aqueous environment can bind. Carbon based materials are activated via treatment alkaline, acidic and basic solution which is a long and arduous procces [7]. Therefore, an efficient functionalization of PET waste should be improved [8]. Elkady let al. 2019, syhenthesized green supported nanoscale zero-valent iron composites for enhanced acid blue-25 dye synergistic decolorization [9]. Ali et al., 2016, developed microwave assited highly efficient superparamagnetic catalyst [10]. Elkady

*Abbrevitations:* nZVI, nano zero valent iron particles; WPET, waste PET bottles (polyethylene terephthalate); MW, microwave energy; WPET-nZVI, nano iron immobilized waste pet bottle; MW/WPET-nZVI, The synthesized WPET-nZVI was subject to heating via microwave; TC, Tetracyclines; FTIR, Fourier Transform Infrared Spectroscopy; EDX, Energy dispersive X-Ray; XRD, X-Ray Diffraction; SEM, Scanning Electron Microscopy.

* Corresponding author at: Cumhuriyet University, Faculty of Engineering, Chemical Engineering Department, 58140 Sivas, Turkey.
*E-mail addresses:* mersan@cumhuriyet.edu.tr, gorgun7@hotmail.com (M. Ersan), hatice.dgn.2016@gmail.com, h.dgn2017@hotmail.com (H. Dogan).

https://doi.org/10.1016/j.colcom.2021.100416
Received 8 February 2021; Received in revised form 13 April 2021; Accepted 13 April 2021
Available online 6 May 2021

et al., 2017 developed microwave assisted superparamagnetic nanocomposite [11] and Songlet al. 2020 investigated N,P-codoped mesoporous carbons (P/NMCs) using liquor grains as the carbon source [12]. Nano zero violent $Fe^0$ derivative from $FeCl_2.4H_2O$ (nZVI) preference of adsorbent, due to wide surface area, enhanced adsorption characteristics, nano-scale dimensions, high density and the high internal reactivity of the surface areas [13,14]. The magnetic effect of nZVI present in the environment results in flock formation and reactivity loss [15]. A supporting material should be used for nZVI in order to prevent such problems. Substances such as zeolite [16], activated carbon [17] have been used in literature to overcome these issues. Hence, WPET-nZVI synthesized by immobilizing nano zero-valance iron and developed via microwave heating assistance.

Active carbons prepared by heat treatment; conventional (conduction, convection, radiation) or microwave heating. Since microwave heating provides features such as rapid volumetric heating, high reaction rate, selectivity, short reaction time and high yield compared with traditional heating methods, microwave application in the synthesis of adsorbents used in many areas has attracted in recent years. Particles are heated up quickly during microwave heating/activation of carbon-rich samples and leading to a significant decrease in volatiles such as hydrogen, oxygen, and sulphur thereby enriching the fixed carbon content of the samples [18]. In addition, it can be defined as an environment friendly and modern heating method that enables heating without decomposition of reactives and without the need for a solvent. Microwave is radiation with wavelength varying in the 1 $m^{-1}$mm interval and frequency varying between 300 GHz and 300 MHz which spreads out in the form of electromagnetic waves. The spreading waves are charged with electricity and the molecule structure of heated matter does not degrade. Heating is due to the dipole moment and electrical fields of matter. This has led to further investigation by establishing the reliability of microwave heating as an alternative activation method to the traditional heating method [19].

Electric and magnetic field configuration of the parallel wire transmission line showed that S. 1. [20]. The importance of microwave energy in adsorption has been emphasized in many studies in literature for increasing adsorbent efficiency. It has been reported that microwave pre-treatment adsorbent has greater pore area and adsorption capacity compared with standard adsorbent and that the MW procedure confers adsorbents with superior features [21]. Hence, WPET-nZVI synthesized by immobilizing nano zero-valance iron was subject to microwave procedure at different durations for increasing adsorption capacity and MW/WPET-nZVI was obtained. New adsorbents Active carbon sources adsorbents WPET, WPET-nZVI and MW/WPET-nZVI were synthesized for the experimental studies conducted in batch system after which the impact of the parameters investigated for tetracycline removal from aqueous solutions.

Tetracyclines are wide-spectrum antibiotics that are frequently used in pharmaceutical industry. Tetracycline (TC), oxytetracycline (OTC) and chlortetracycline (CTC) are used in many countries to preserve the health of animals and to promote growth. These chemicals are characterized by the four ring structure partially conjugated with the carboxamide functional group [22]. Open formula of the tetracycline molecule is presented in Fig. S.2. [23]. Tetracyclines (TCs) are antibiotics that are frequently used in the treatment of people, animals and plants [24]. They are known to be severely toxic on humans and other living organisms [25]. TC in the environment results in resistant microorganisms and leads to severe environmental pollution by threatening human health through an increase in the risks involved with various infections [26]. Since the majority of the structure consists of waste water and aromatic rings, the frequent use of tetracyclines results in significant damages by making an adverse impact on the environment and ecosystem with the carcinogenic substances they contain. Hence, measures are continued to be taken to minimize the levels of damage and risk [27]. Tetracycline is quite resistant against biodegradation processes and they are not generally biodegraded in classical treatment plants. Traditional methods used for TC removal from wastewaters are known as oxidation [28], active sludge, coagulation and flocculation [29], graphitic carbon adsorption [30], membrane technology [31]. Adsorption is an efficient, simple and low cost removal technique. Recently, scientists conducted studies on the synthesis of new and cheap adsorbents. Adsorption is a good method for the removal of TC from wastewater [32]. The medium pH and presence of electrolytes considerably affected TCs adsorption on commercial activated carbon and these results indicate that electrostatic adsorbent–adsorbate interactions play an important role in TC adsorption processes when conducted at pH values [33]. It was reported that highly efficient materials for TC removal at literature. For example; adsorbents were developed using activated carbon or their composites supported nZVI and MW treatment adsorbents [34,35].

The aim of the this study was to undarstund the removal of TC from wastewater using green syhenthesis WPET, WPET-nZVI (magnetic adsorbent) and MW/WPET-nZVI (magnetic and MW pre-treatment adsorbent). The syhenthesis of the environmental friendly adsorbents characterization, effect of various parameters on the removal process, kinetic studies of the adsorption process; adsorption isotherms and thermodynamic parameters, and possible removal mechanisms are reported in this study.

## 2. Experimental

### 2.1. WPET-nZVI synthesis

The waste PET bottles used in the study were reduced in size down to 1–5 mm after which they were subject to carbonization in closed stainless steel reactor kiln under vacuum. Carbonization procedure was carried out at 280 °C for 2 h after which the bottles were left to cool took 24 h. The obtained dark colored carbonization products were ground (−53 μm) to obtain WPET. While preparing the Nano valence iron immobilized WPET-nZVI; 24 mL ethanol was taken for the first solution and filled up to 30 ml with distilled water. Afterwards, 5.34 g $FeCl_2.4H_2O$ was added followed by the addition of WPET obtained from 1.5 g waste polyethylene terephthalate. 3.05 g $NaBH_4$ was weighed for the second solution and filled up with 100 ml distilled water. These prepared solutions were mixed in a mixer for 5 in. Afterwards, the second solution was poured drop by drop to the first while the first solution was being mixed thus obtaining a black and viscous solution. The solution obtained as such was centrifuged at 4000 rpm (Hettich universal). The centrifuged adsorbents were filtered through a blue band filter paper and washed 2–3 times with ethanol. The obtained WPET-nZVI was stored in a closed medium after drying for 3 h at 50 °C in a drying oven. The amount of samples required for the experiment was heated in microwave for 2 min at 600 W thus obtaining MW/WPET-nZVI (S. 3).

### 2.2. Microwave pre-treatment for WPET-nZVI

WPET-nZVI adsorbents were placed in a glass and oval plate after which they were heated in a BOSH OM-439 microwave oven at 600 W power for 2 min obtaining MW/WPET-nZVI materials. The 10 g/l adsorbent to be used in the experiment was placed on a glass material as pre-treatment after which microwave heating pre-treatment was applied for 2 min at 600 W.

### 2.3. Batch system studies

Batch experimental studies were conducted in sterile Erlenmeyer flasks with a working volume of 100 ml at constant temperature and 180 rpm stirrer. Stock TC solution was used by diluting to the desired concentrations in tetracycline adsorption studies. Required amounts were taken from tetracycline antibiotic (1 g) after which stock tetracycline solution was prepared at 1000 mg/l concentration and 1l volume.

TC stock solution was prepared at frequent intervals against any form of decomposition and was stored in a dark environment. Different TC concentrations were obtained by way of required dilutions from the stock antibiotic solution. Starting experiments were conducted in order to determine the optimum pH value in adsorption studies. Whereas 0.1 M NaOH and $H_2SO_4$ solutions were prepared and used for adjusting the pH value of the solutions. WPET, WPET-nZVI and MW/WPET-nZVI were used as adsorbent when removing tetracycline from the aqueous solution. WPET-nZVI was prepared and experiments were conducted at 20 °C and 180 rpm mixing speed with initial TC concentrations of 10, 25, 50, 75, 100, 150, 200 mg/l. MW/WPET-nZVI immobilize adsorbent subject to adsorbent microwave procedure along with 5 ml samples taken at specific time intervals (5, 15, 30, 60, 90, 120, 180, 240 min) and different temperatures (20, 30, 40 °C) were centrifuged at 4000 rpm for 10 min followed by reading the absorbance value at $\lambda_{max}$ 357 nm and analysis in UV device [36].

### 2.4. Kinetic studies

Adsorption process has been evaluated through kinetic studies for the investigation of its rate and mechanism. The pseudo-first-order and pseudo-second-order and intraparticle diffusion models were applied which are specified in Eq. (1–3).

$$\text{Pseudo} - \text{first} - \text{order} : ln\ (q_e - q_t) = ln\ q_e - k_1 t \quad (1)$$

$$\text{Pseudo} - \text{secon} - \text{order} : k_2\ q_e^{\ 2}\ t/1 + k_2\ q_e\ t \quad (2)$$

$$\text{Intraparticle diffusion} : q_t = k_i\ t^{1/2} + I \quad (3)$$

Where, $q_e$ (mg/ g); amount of TC adsorbed at saturation per gram of adsorbent, $q_t$ (mg/ g); the amount of antibiotic adsorbed at time t per gram of adsorbent, $k_1$ ($min^{-1}$); the rate constant of the pseudo first-order adsorption, $k_1$ and $k_2$; pseudo-first-order and pseudo-second-order adsorption rate constants, respectively, $k_i$ (mg/ g $min^{-1/2}$); intraparticle diffusion rate constant, I; constant for boundary layer or mass transfer effect [37].

### 2.5. Adsorption studies

Many researchers are striving to find cheap and renewable adsorbents in order to render the adsorption process more effective and less costly. Mathematically, this equilibrium is explained by way of adsorption isotherms. The most general isotherms are Langmuir, Freundlich D-R and Temkin isotherms (Eqs. 4–9) were given Table 1.

**Langmuir isotherm:**

Where; $\alpha_L$;is the constant dependent on adsorption energy ($dm^3$/mg), $Q_{max}$; denotes the monolayer adsorbent capacity (mg/l) [38].

$$\text{Langmuir isotherm} : qe = \frac{Q_{max}\alpha_L C_e}{1 - \alpha_L C_e} \quad (4)$$

**Freundlich isotherm;**

**Table 1**
Adsorption kinetic models paremeters for TC Removal by the 2 min/WPET-nZVI.

| | | |
|---|---|---|
| Experimental $q_e$(mg/g) = 4.75 | *Pseudo first order* | |
| | $R^2$ | 0.9825 |
| | $k_1$ ($min^{-1}$) | 0.0133 |
| | $q_e$ (mg/g) | 0.503 |
| | *Pseudo second order* | |
| | $R^2$ | 0.9998 |
| | $k_2$ (g/mg.min) | 0.1002 |
| | $q_e$ (mg/g) | 4.76 |
| | h (mg/g.min) | 2.26 |
| | *Intraparticle diffusion model* | |
| | $R^2$ | 0.9673 |
| | $k_d$ (mg/g.$min^{0,5}$) | 0.0344 |
| | I | 4.2345 |

Where; $q_e$ denotes the amount of substance adsorbed on unit adsorbent (mg/g), $C_e$; paint concentration remaining in the solution after adsorption (mg/l), $K_F$; adsorption capacity (l/mg) and n represents adsorption density [39].

$$\text{Freundlich isotherm; qe} = \frac{\text{KFCe1}}{\text{n}} \quad (5)$$

**D-R (Dubinin-Radushkevich) isotherm:**

Used for systems for which the characteristic adsorption curve is subject to the porous surface of the adsorbent. Where; $q_{D\text{-}R}$ denotes the maximum adsorption capacity (mol/g), β; D-R represents the model constant ($mol^2$ / $J^2$), ε is the Polanyi potential (J/mol) and E represents the average adsorption energy (kJ $mol^{-1}$). E value gives an idea on the type of adsorption. Ion exchange is observed for $8 < E < 16$, physical change is observed when $8 < E$ and chemical change is observed when $E > 16$ [40].

$$\text{D} - \text{R isotherm} : E = \frac{1}{\sqrt{2\beta}} \quad (6)$$

$$qe = q_{D-R} e^{-\beta\varepsilon^2} \quad (7)$$

$$= RTln\left[1 - \frac{1}{C_e}\right] \quad (8)$$

**Temkin adsorption isotherm**

Temkin isotherm model takes into consideration the indirect effects of the adsorbed-adsorbent interaction isotherms indicating that the adsorption heat of all molecules on the adsorbent surface layer will decrease linearly with the area affected by the adsorbed-adsorbent interactions. The slope of the line drawn by plotting the lnCe values against qe values gives the bT constant and its intercept gives bT lnkT. Where; $q_e$ denotes the equilibrium adsorption capacity ($mgg^{-1}$); $b_T$ represents the Temkin isotherm adsorption energy (j g/mol mg) and $K_T$ denotes the Temkin isotherm constant (l/mg) [41].

$$\text{Temkin adsorption isotherm} : q_e = b_T ln K_T - b_T ln C_e \quad (9)$$

### 2.6. Thermodynamic studies

Thermodynamic parameters and $K_d$ as the equilibrium partition constant were calculated by the following equations of Eq. 10–13. Where, ΔG (kJ $mol^{-1}$) is the Gibbs free energy change, $K_d$ denotes the equilibrium partition constant, T (K) represents the temperature, ΔH (kJ $mol^{-1}$) is the enthalpy change and ΔS (kJ $mol^{-1}$ $K^{-1}$) denotes the entropy and R (8.314 J/mol $K^{-1}$) is the universal gas constant. The values of ΔG were calculated from the K values for each temperature, the values of ΔH and ΔS were calculated from the slope and intercept of the plot of ln $K_d$ versus 1/T, respectively [1].

$$\Delta G^0 = \Delta H^0 - T\Delta S^0 \quad (10)$$

$$Kd = \frac{C_e}{q_e} \quad (11)$$

$$\Delta G^\circ = -RTlnK_d \quad (12)$$

$$ln Kd = \frac{\Delta S^0}{R} - \frac{\Delta H^0}{RT} \quad (13)$$

## 3. Results and discussions

### 3.1. Characterization of adsorbents

FTIR spectroscopy was used in order to identify the functional groups of the waste PET adsorbent to be used as adsorbent. FTIR (Fourier transform infrared spectroscopy) spectroscopy is a frequently used analytical method for identifying the molecule structure based on the

vibration characteristics of the chemical functional groups in a molecule. In addition, it can be examined based on the vibration bands whether the adsorption process took place or not by making use of the vibration movements in the adsorbent after TC adsorption. There are applications in literature with examples of FTIR use for examining TC removal before carbonization and after adsorption [42]. Strain, shortening and folding movements are observed on the chemical bonds present with the interaction of the nZVI, WPET, WPET-nZVI, 2 min WPET-nZVI and after TC adsorption 2 min WPET-nZVI materials subject to spectrums measurement for adsorbents and infrared light. Chemical functional groups start absorbing via infrared light interaction in a specific wavelength interval independent of molecule structure. FTIR spectra were scanned in order to examine the surface structure prior to TC adsorption via WPET which are presented in Fig. 1.

The 3200–3600 $cm^{-1}$ peak resulted from the O—H bonding for all adsorbents however there is no peak in this range due to the burning process of WPET. The range of 682–1706 $cm^{-1}$ peaks were obtained for adsorbents due to structural differences related with iron oxides. These bands that are smaller than 1345 $cm^{-1}$ in the nZVI modified adsorbents result from the reduced oxidation of immobilized $Fe^0$ [31]. The bands of 2350.07 $cm^{-1}$–2324.37 $cm^{-1}$ and 2114.48 $cm^{-1}$ in the pre-adsorption FTIR spectra of WPET are due to the asymmetric vibration of $CH_2$ and indicate the presence of $CH_2$ and $CH_3$ aliphatic hydrocarbon groups. There are three or four C═C strain vibration bands between 1450 $cm^{-1}$-1600 $cm^{-1}$ in aromatic compounds. The peaks in the wavelength interval of 1200–1700 $cm^{-1}$ signify the presence of benzene rings. Whereas the 1596.55 $cm^{-1}$ band corresponds to the stretching vibration of the peptide bonds of proteins COO, C═O and C—N (amide I) [43]. Whereas the 1431 $cm^{-1}$ band is the stretching vibration of phenolic -OH and carboxylate C═O while 1230.83 $cm^{-1}$ band corresponds to the vibration of epoxy C-O-C and carboxylic acids. 1183.72 $cm^{-1}$ band corresponds to the alkoxy C—O vibration [44]. 756.13 $cm^{-1}$ and 656.97 $cm^{-1}$ have indicated aromatic representation bending and the presence of outer-plane adjacent aromatic CH hydrogens [45]. It was observed when FTIR spectra were examined after MW /WPET-nZVI TC adsorption that the 3390.55 $cm^{-1}$ peak emerged following the application of the microwave process thus enabling the formation of a more stable structure due to the removed H and O molecules. Thus, it was concluded that nano iron immobilization and microwave heating processes are effective on carbonization and that increasing adsorption capacity increases TC adsorption efficiency as well.

The XRD diagrams is used to identify the crystalline structure and XRD patterns of 2 min MW/WPET-nZVI are shown in S-4. The XRD pattern of the material indicates that the principal components of this material include graphen magnetite ($Fe_3O_4$) which are synthesized by precipitation and microwave technology [5]. X-ray diffraction peaks were observed at 16.80, 27.09 and 47.01 2θ. The 16.80 peak is due to the presence of micropores and TC molecule structures. 2θ values of 27.09, and 47.01 which are FeO(OH) covered graphitic material [46]. This results showed that nZVI syhenthesized succesfuly and WPET covered FeO(OH).

Another characterization method for adsorbents is Energy-dispersive X-ray spectroscopy (EDX) which is an analytical technique used for the elemental analysis or chemical characterization of a sample. Fig. 2. presents the EDX analysis of the synthesized 2 min MW/WPET-nZVI. The results show the synthesized 2 min MW/WPET-nZVI, elemental analysis was conducted with 17.91% Fe, 11.60% C and 63.94%. It can be deduced that the adsorbent was covered with Fe and that $H_2O$ decomposed into H and O following MW treatment.

Scanning Electron Microscope (SEM) was used to examine the surface properties of the synthesized adsorbents. Fig. 3. shows the SEM images for nZVI (a), nZVI immobilized WPET-nZVI (b) and MW/WPET-nZVI subject to microwave process for 2 min (c) and MW/WPET-nZVI for after TC adsorption process (d). It can be understood when the SEM images are examined that the pore structure of iron is smaller than other adsorbents. nZVI modified WPET and carbonic structure form magnetic rods (b), that pore size and number increased after the microwave process (c) and that TC is adsorbed on the pores (d).

### 3.2. pH effect on TC removal with WPET

The pH value of the solution is one of the most important parameters with an impact on pollutant removal. The effect of pH on tetracycline removal from PET bottle waste was examined at an initial pH interval varying between 3 and 8. The experiments were conducted at 20 °C with 50 mg/l initial tetracycline concentrations and 10 g/l adsorbent concentration.

Fig. 4(a) presents the impact of pH on the adsorption capacity of waste PET used as adsorbent in TC removal. Tetracycline removal

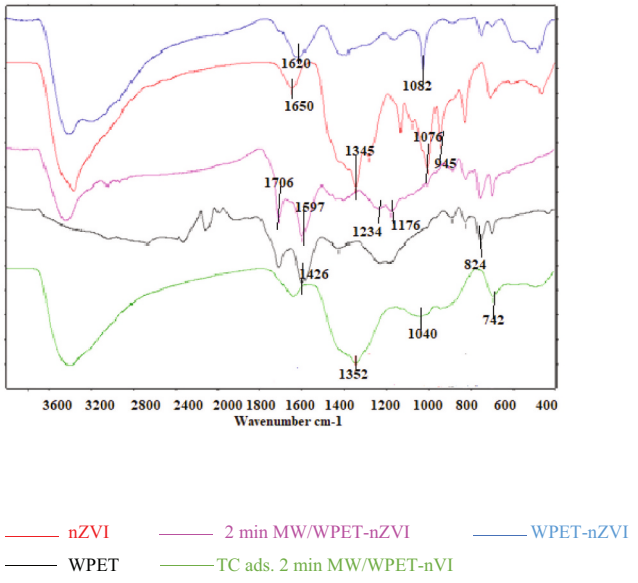


**Fig. 1.** FTIR spectra of adsorbents and after TC adsorption 2 min MW/WPET-nZVI.

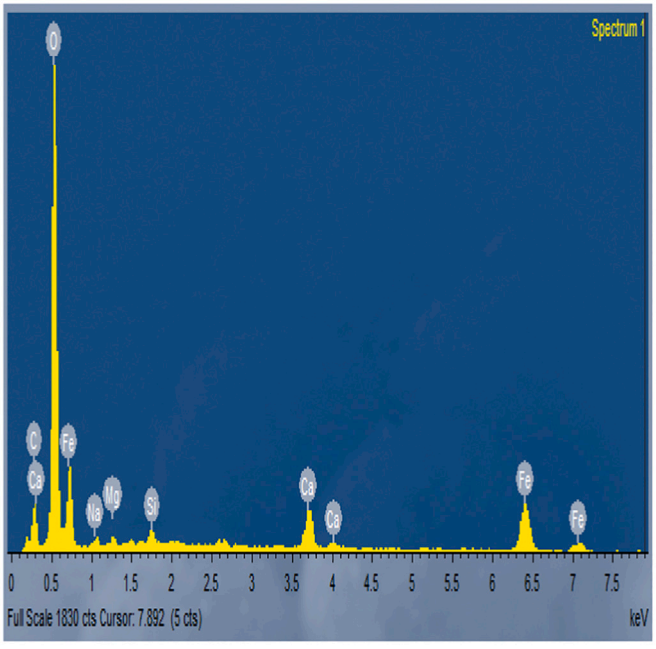


**Fig. 2.** Energy dispersive X-Ray (EDX) analysis of the 2 min MW/WPET-nZVI.

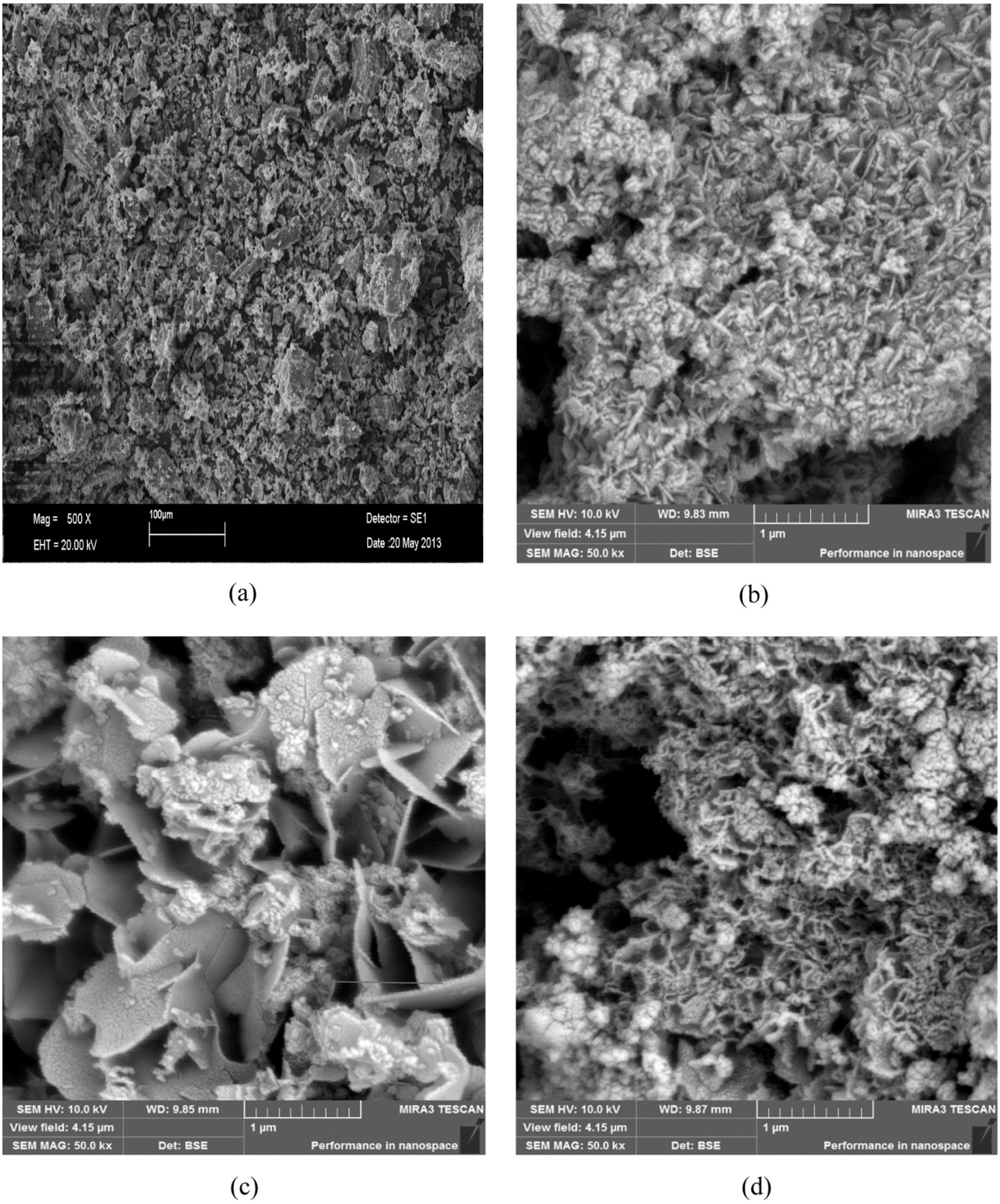


**Fig. 3.** SEM Images a) n-ZVI b) WPET-nZVI c) 2 min MW/WPET-nZVI d) After TC adsorption 2 min MW/WPET-nZVI.

increased with increasing initial medium pH with the highest removal yield obtained as 92.42% at pH 4 (a). TC removal yield increased between pH 3 and 5 due to the weak electrostatic repulsive force. TC removal efficiency decreased by the use of WPET in the pH 5 to 9 range interval due to the impact of different mechanisms such as attributed to complexation interactions, electrostatic interactions, ion exchange, cation–π bonding, and π–π EDA interactions in addition to electrostatic repulsive forces [45]. The higher is the pH (higher than 7) value, the lower % removal will be which may be due to the repulsion forces between ($OH^-$) from TC groups as well as the adsorbent surface which has an adverse impact on removal efficiency [46].

In this situation, the decrease in removal efficiency may be explained by electrostatic repulsion between surface areas and TC molecule. The effects of pH on the TC removal rates and the zero point of charge (pHpzc) are presented in Fig. 4(b), whereas, at pH solution pH (2–4–6–8–10) was studied using a 100 mL solution containing 50 mg TC/l. pHpzc value of WPET was found to be approximately 7.02 [47]. pH value at optimum conditions was lower than the pHpzc of WPET, the composites surface was positively charged. The adsorption of ions is affected from whether the medium where adsorption takes place is

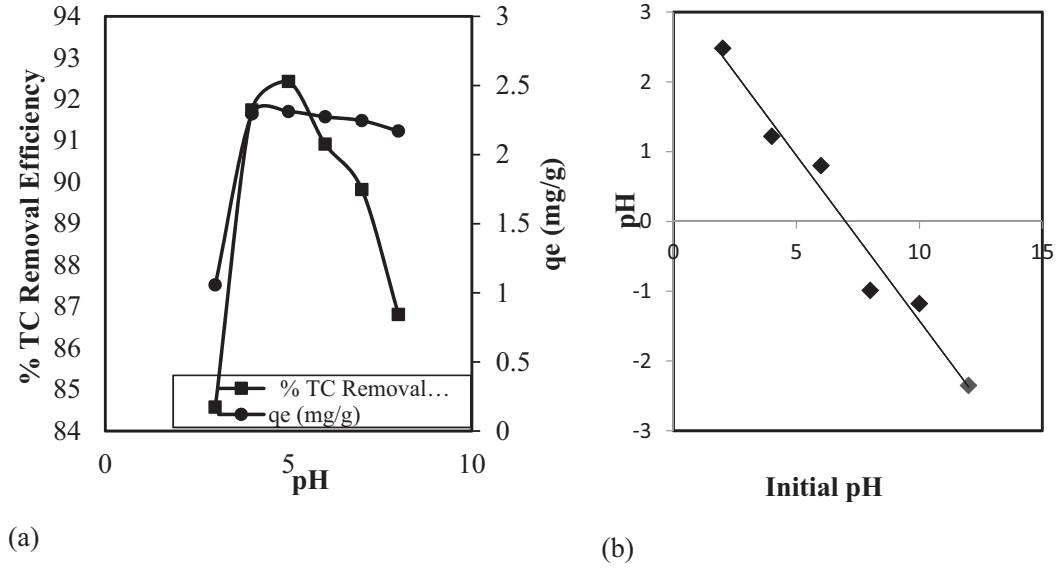


**Fig. 4.** (a) pH effect on TC removal with WPET, (b) Variation of ΔpH versus initial pH for the determination of point of zero charge (m = 10 g/l, $C_0$ = 50 ppm, $T$ = 20 °C, 180 rpm and 2 h).

acidic or basic, that is from the strong adherence of H- and OH- ions to the surface as well as from the pH values of the solution. Tetracycline molecule can be present in 3 forms subject to the pH value. It is in cationic form for pH˂3.3, in dipolar (zwitter) ion form for 3.3˂pH˂7.7 and negatively charged when pH˃7.7. Tetracycline is neutral for pH values of 3.3–7.7 and negative for pH values of greater than 7.7. Electrostatic interaction should be weak at low pH, because OH / COOH protonation on WPET makes WPET less negative. The removal mechanism might be via surface complexation and/or cation exchange on the surface sites. The pH value of the solution where adsorption takes place has a significant effect on the adsorption amount. The adsorption of ions is affected from whether the medium where adsorption takes place is acidic or basic that is the strong adherence of $H^-$ and $OH^-$ ions to the surface and the pH values of the solution. High TC removal efficiency (92.42%) in environments with pH 5 has indicated that adsorption capacity has increased through the establishment of a strong electrostatic force between tetracycline and WPET.

### 3.3. The effect of WPET amount on TC removal

Each of the adsorbent samples at different amounts was treated separately together with their 50 ml TC solutions under specific adsorption conditions (pH = 5, $C_0$ = 50 ppm, $T$ = 20 °C, 180 rpm and 2 h) in order to identify the effect on TC adsorption of adsorbent amount which is a critical factor for the cost effectiveness of the adsorption process. Fig. 5(a) shows the effects of adsorbent amount on TC removal efficiency (%) and adsorption capacity qe (mg/g). TC removal yield increased rapidly at first with the increase of adsorbent amount thus reaching 92.42% at 10 g/l [44]. An increase in adsorption capacity took place since the sudden initial increase in TC % adsorption rate indicates greater surface area and indirectly the presence of more functional bonding centers for adsorption. The increase in the amount of adsorbed pollutant with increasing adsorbent dosage and thus the increase in removal efficiency can be explained by the fact that adsorption is a surface process and that adsorption power is one of the important functions of surface properties. The increase in TC removal is due to the increase in the surface area and the present active surface regions of WPET. TC removal did not result in a significant increase with more WPET dose after an adsorbent dosage of 10 g /l. Hence, high removal efficiency can be attained in porous materials and solids divided up into very small parts for increased surface area [48]. Experiments for WPET-nZVI and 2 min MW/WPET-nZVI adsorbents were conducted at 20 °C with 50 mg/l initial tetracycline concentrations, 10 g/l adsorbent amount and at pH 5 under the same optimum conditions.

### 3.4. Effect of initial TC concentration and MW re-treatment time

Since adsorption rate is a function of initial TC concentration, TC and adsorbent concentration values that determine the asorbent/adsorban balance of the system are important factors that should be taken into consideration [39]. The effect of initial TC concentration on adsorption capacity was examined by conducting tetracycline removal studies at different tetracycline concentration solutions (10–300 mg/l) using the same amount of adsorbent (10 g/l) under conditions of pH = 5, $T$ = 20 °C, 180 rpm and 2 h. The ideal removal yield for WPET was identified at 50 ppm at 92.42%. Therefore, WPET- nZVI which is a magnetic adsorbent was used in the adsorption isotherm studies during which nZVI and its structural properties are used through WPET characterization. Removal efficiency of 93.10% was obtained for WPET-nZVI at 10 g/l. The effect of microwave energy was examined as an alternative to the traditional heating systems for increasing efficiency and the maximum removal yield of 93.38% was obtained with 2 min MW/ WPET-nZVI (Fig. 5(b)). Waste PET, magnetic adsorbent (WPET-nZVI) made with waste PET and three adsorbents obtained as a result of 2 min microwave procedure applied on magnetic adsorbent were compared for constant temperature and initial TC concentration effect was put forth for WPET, WPET-nZVI and 2 min MW/ WPET-nZVI (Fig. 5(c)). The determined pH (5) was kept constant via the adsorbent amount of the substance subject to MW pre-treatment for 2 min (10 g/l), initial TC concentration (50 mg/L), contact time (120 minutes) and temperature (20 °C) thus examining its impact on the adsorption process. There have been a lot of studies in the literature for TC removal for example, TC removal process can discussed $q_{max}$(mg/g) values; pumice stone, 20.02, HA-C, 76.02; nZVI-P-nZVI, 105.46, [36]. In this study TC adsorption capacity of adsorbents ($q_{max}$; mg/g) were found as 67.11, 80.64, 105.26 for WPET, WPET-nZVI and 2 min MW/WPET-nZVI respectively. It is concluded that the removal efficieny is quite high of new adsorbents which are 'green syhenthesized' basic, when these result compared with literature.

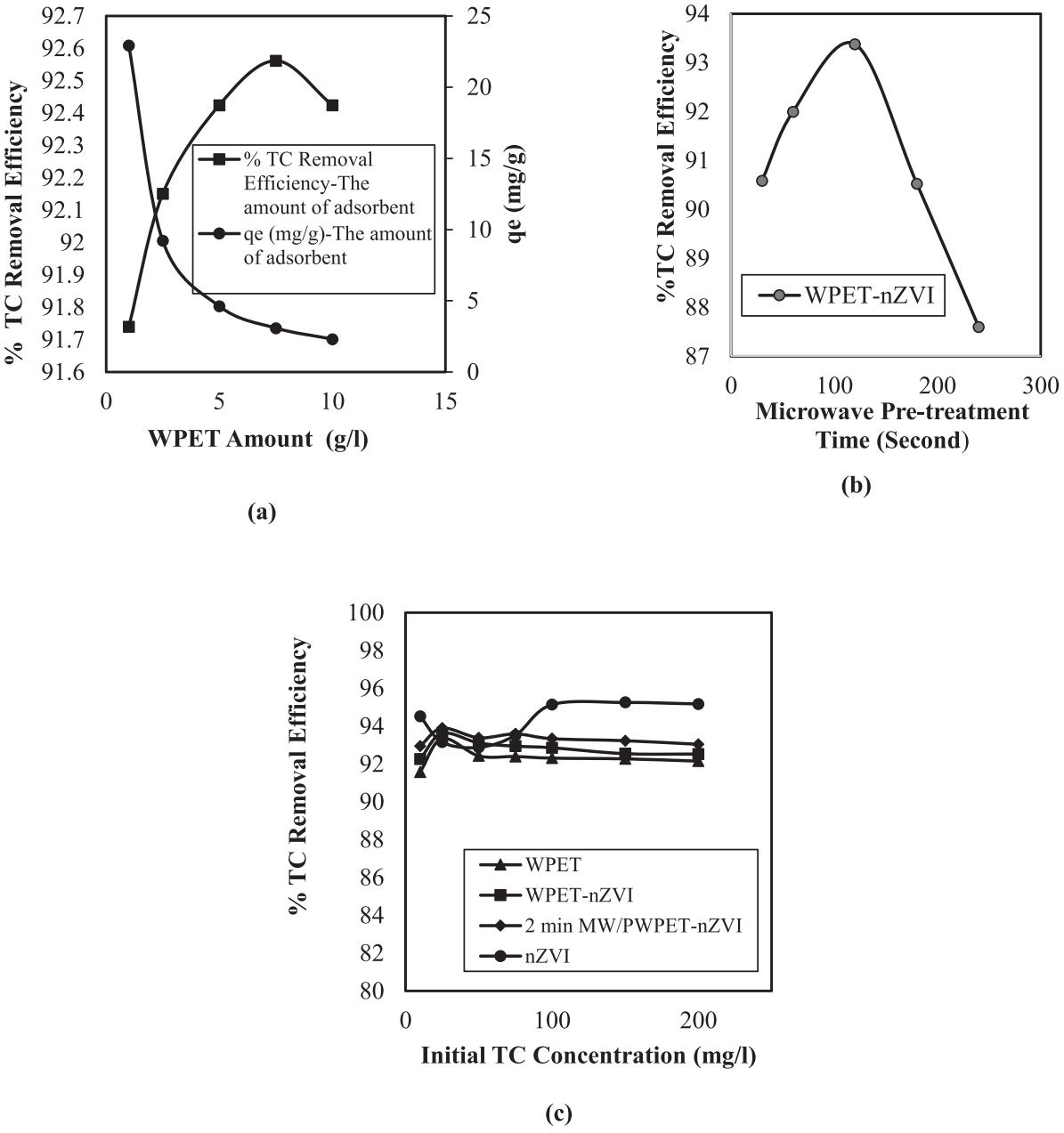


**Fig. 5.** (a). The effect of WPET amount on TC removal, (b) The effect of microwave pre-treatment time on WPET-nZVI efficiency, (c) The effect of initial TC concentration (pH = 5, m = 10 g/l, $T$ = 20 °C, 180 rpm and 2 h).

### *3.5. Kinetics, isotherms and thermodynamic studies of adsorption process*

The effect of contact time on TC adsorption on 2 min WPET-nZVI was investigated in the range of 5–240 min for the initial concentration of 50 mg/l for TC molecule and kinetics were calculated. The experimental and theoretical qe values were calculated as 4.75 mg/g and 0.503 mg/g respectively with a discrepancy. However, the correlation coefficient of the pseudo-second-order kinetic model $R^2$ was found to be the closest to 1 with a value of 0.9998. The value of qe calculated via pseudo-second-order kinetic model was 4.76 mg/g and theoretically, the suitability was proven when qe was calculated as 4.75 mg/g (Table 1). The pseudo-second-order model is empirically the most compatible. Sufficient linearity was reached for intra-particle diffusion. $R^2$ yielded a high value of 0.9673. Analysis and comparison of TC adsorption parameters on 2 min/WPET-nZVI were conducted and defined by way of a pseudo-second order model. The pseudo-second-order kinetic model assumes that the rate-controlling step may be chemisorptions involving valency forces exchanging of electrons between TC and 2 min/WPET-nZVI and faster at the higher temperatures [10].

The highest adsorption removal efficiency was determined as 93.38% in Fig. 5b at an initial concentration of 50 mg/l. Langmuir, Freundlich, D-R and Temkin adsorption isotherm models were used in the present study for defining the adsorption equilibrium. Table 2 shows TC, Langmuir, Freundlich, D-R and Temkin adsorption isotherm parameters for WPET, WPET-nZVI and 2 min MW/WPET-nZVI. Figs. 6 (a, b, c, d), show the linearized figures of the isotherm graphs.

The slope and intercept of the line in Langmuir isotherm graph are used for calculating the values of the Langmuir constants for each adsorbent in mg/g and l/mg as $q_{max}$ (maximum adsorption capacity for the adsorbent) and energy constant b related with adsorption heat. In the meantime, the $q_{max}$ values of three adsorbents were sufficient for observing the strong impact of the microwave procedure on the

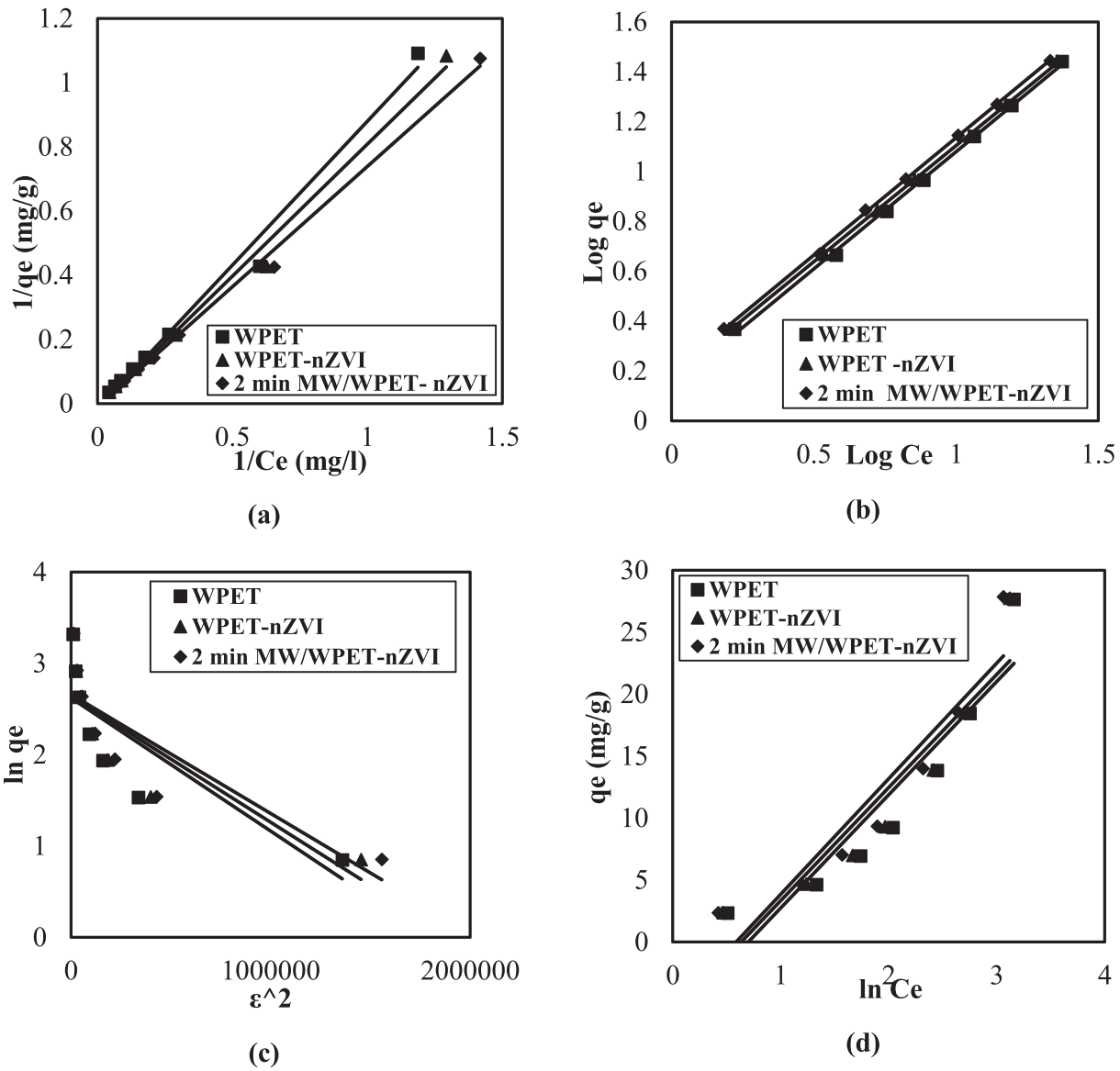


**Fig. 6.** (a) Linearized Langmuir isotherm, (b) Linearized Freundlich isotherm, (c) Linearized D-R isotherm, (d) Linearized Temkin isotherm (pH = 5, m = 10 g/l, $C_0$ = 50 ppm, $T$ = 20C, 180 rpm and 2 h).

adsorbents (Fig. 6(a)). The slope of the line in the Freundlich isotherm graph was used for calculating the $1/n$ values which are indicators of adsorption intensity or surface heterogeneity and cut off value was used for calculating the $K_f$ value which is an indicator of adsorbent capacity (Fig. 6(b)). High $K_f$ value, values of $1/n < 1$ or $n > 1$ and high regression constant ($R^2$) values indicate that the compliance of the experiment data with the Freundlich isotherm is quite high [44]. The applicability of both Langmuir and Freundlich isotherms on the adsorption of TC on MK and synthesis materials indicate that the adsorption is monolayered and takes place under heterogeneous surfaces. Maximum adsorption capacities have been determined in the Langmuir model $q_{max}$ values were determined as 67.11 mg/g, 80 mg/g and 105.26 for PET bottle waste, WPET-nZVI and 2 min MW/WPET-nZVI. Table 3.1 presents the value of the adsorption energy constant β from the intercept of the Dubinin–Radushkevich (D–R) isotherm line formed by the linearization of lnqe values against $E^2$ in addition to the adsorption capacity of the adsorbent $q_{D\text{-}R}$ from the intercept. In addition, adsorption energy (E) was calculated by using the adsorption energy constant in the related equation (Fig. 6(c)). High $R^2$ value in the Temkin isotherm indicates that the adsorption heat of all models on the adsorbent surface layer will decrease linearly with the area affected by the adsorbed–adsorbent interactions (Fig. 6(d)). In addition, very high values of the Langmuir b constant indicating the adsorption energy is an indicator of the higher adsorption energy that manifests itself with a rapid increase in adsorption at low adsorbent concentrations.

### 3.6. Determination of thermodynamic parameters

To define the thermodynamic parameters of the system, experiments were managed at different temperatures; 25, 35 and 45 °C., pH 5, adsorbent dosage 2 min WPET-nZVI at 10 g/l, initial TC concentration 50 mg/l and contact time 120 min. It was observed that as removal efficiency was 93.38% at 25 °C with increasing temperature (S.5). Thermodynamic parameters, Gibbs free energy ($\Delta G^0$), enthalpy ($\Delta H^0$) and entropy ($\Delta S^0$), are shown in Table 2. It was observed that the adsorption efficiency decreased with increasing temperature. This is due to the fact that the forces of attraction between the solute and the surface decrease with increasing temperature. Gibbs free energy ($\Delta G^0$), one of the thermodynamic parameters, values were negative and very close. Negative values of ($\Delta G^0$) 'indicate that adsorption occurs spontaneously. The

**Table 2**
Langmuir, Freundlich, D-R and Temkin adsorption isotherms and thermodynamic parameters for WPET, WPET-nZVI and 2 min MW/WPET-nZVI).

| | | | | |
|---|---|---|---|---|
| *WPET* | | | | |
| **Langmuir Model** | | **Freundlich Isotherm** | | |
| $q_{max}$ (mg/g) b (l/mg) $R^2$ | | $K_F$ (l/g) 1/n $R^2$ | | |
| 67.11 0.021 0.9957 | | 1.37 0.9398 0.9987 | | |
| **D-R Model** | | **Temkin Model** | | |
| $q_{D\text{-}R}$ (mol/g) E (kj/mol) β($mol^2/j^2$) $R^2$ | | $b_T$ (j g/mol mg) $K_T$ (l/mg) $R^2$ | | |
| 13.74709.2 $1.10^{-6}$ 0.6978 | | 9.1382 0.7 0.8614 | | |
| *WPET-nZVI* | | | | |
| **Langmuir Model** | | **Freundlich Isotherm** | | |
| $q_{max}$ (mg/g) b (l/mg) $R^2$ | | $K_F$ (l/g) 1/n $R^2$ | | |
| 80 0.0186 0.9986 | | 1.48 0.9311 0.9998 | | |
| **D-R Model** | | **Temkin Model** | | |
| $q_{D\text{-}R}$ (mol/g) E (kj/mol) β($mol^2$/j2) $R^2$ | | bT (j g/mol mg) $K_T$(l/mg) $R^2$ | | |
| 14.05709.2 $1.10^{-6}$ 0.7183 | | 9.1303 0.635 0.8713 | | |
| *2 min MW/WPET-nZVI* | | | | |
| **Langmuir Model** | | **Freundlich Isotherm** | | |
| $q_{max}$ (mg/g) b (l/mg) $R^2$ | | $K_F$ (l/g) 1/n $R^2$ | | |
| 105.26 0.014 0.9987 | | 1.56 0.9418 0.9996 | | |
| **D-R Model** | | **Temkin Model** | | |
| $q_{D\text{-}R}$ (mol/g) E (kj/mol) β($mol^2/j^2$) $R^2$ | | bT (j g/mol mg) $K_T$(l/mg) $R^2$ | | |
| 23.43158.73 0.002 0.9011 | | 9.3274 0.587 0.8816 | | |
| *Thermodynamic Parameters (kJ $mol^{-1}$)* | | | | |
| $\Delta H^0$ | $\Delta S^0$ | $\Delta G_1^0$ | $\Delta G_2^0$ | $\Delta G_3^0$ |
| −278.21 | 49.28 | −14,406.78 | −146,653.62 | −15,146.421 |

positive value of $\Delta S^0$indicates that the irregularity increases at the layer / liquid interface during the adsorption process. It is demonstrated that TC molecules need to substitute the water molecules on the adsorbent surface [37]. The adsorption process of TC yields negative $\Delta H^0$ and $\Delta G^0$values for the adsorbent. The negative values indicate that the adsorption process is exothermic and spontaneous.

### 3.7. Adsorption mechanism

Adsorption mechanism may be influenced by various factors such as weak and strong interactions.The optimum removal yield for WPET, WPET- nZVI and WPET-nZVI were identified as, 92.42%, 93.10, 93.38 respectively. These results showed that magnetic WPET more effective than WPET. Moreover, microwave energy contributes to adsorption by increasing to movement of molecules and magnetic effect of ions. Binding mechanisms and comparison of WPET, WPET-nZVI and MW/WPET-nZVI with other adsorbents may lead to adsorption process through two mechanisms. In general, the TC adsorption by 2 min WPET-nZVI was achieved; the rapid external surface adsorption for initial 20 min and the slow intraparticle diffusion (20–150 min). (i) The adsorption of TC molecules to the surface of the adsorbents might be due to formation of hydrogen bonding between TC molecules and surface. (ii) The second possible mechanism might be that the TC molecules on Fe coated adsorbent surface bond with those on H—Fe [36]. Fe(*O*)OH adsorbent surface was coated after which $TC_xFe$ (1-x)$OH_3$ complexes were formed following the adsorption process. The second mechanism also included the first mechanism with a higher WPET-nZVI performance compared with WPET. Microwave pre-treatment WPET-nZVI active the H binding for the adsorbent and increased the binding capacity. (iii) High regression value (0.9673) results of the intraparticle diffusion model showed that the adsorption process is supported by difussion. Intraparticle diffusion model was explained to transport of TC molecules in the bulk solution, film diffusion of TC at the boundary layer or diffusion of charged molecules from bulk solution to external surface and TC diffusion via small pores of 2 min /WPET-nZVI [37]. Possible reactions and mechanism equations; adsorption, oxidation in acidic solution, oxidation at basic solution, oxidation at acidic solution and reduction (for MW treatment adsorbents highly effective) are given respectively as follows Eqs. (13–17):

$$TC + nZVI, WPET - nZVI \text{ or } 2\ min(WPET - nZVI) \rightarrow TC - nZVI, TC - WPET + -nZVI \text{ or } 2\ min(MW) - nZVI \quad (13)$$

$$TC + F^{(0)} + 2H^{(1+)} \rightarrow Fe^{(2+)} - TC + 2e^{(-)} \quad (14)$$

$$TC + F^{(0)} + 2H_2O \rightarrow Fe^{(2+)} + H_2 + 2OH^{(-)} - TC + 2e^{(-)} \quad (15)$$

$$TC + 2F^{(2+)} + 2H^{(+)} + 1/2\ O_2 \rightarrow Fe^{(3+)} - TC + H_2O \quad (16)$$

$$nTC + (1-x)e^{(3+)} + 3H_2O \rightarrow TC_nFe(1-n)(OH)_3 + 3H^{(+)} \quad (17)$$

## 4. Conclusion

In the present study; nZVI magnetic adsorbent was modified to WPET, WPET-nZVI and MW/WPET-nZVI adsorbents to produce WPET-nZVI synthesis materials. Highest efficiency values were determined for WPET, WPET-nZVI and 2 min MW/WPET-nZVI as; 92.42%, 93.10%, 93.38% respectively. TC removal efficiency was obtained as 93.38% experimentally under optimum experimental conditions (temperature 20 °C, MW duration 2 min, initial TC concentration 50 mg/l). Characterization studies, after TC adsorption were conducted for 2 min MW/WPET-nZVI with the highest TC removal efficiency after which the properties of the synthesized adsorbents were examined and it was observed from the FTIR spectra that the properties of the nZVI immobilized on WPET changed as a result of the microwave applied on the adsorbent resulting in peak shifts and that a more stable structure was formed with TC adsorption. In conclusion, a low cost, easily obtainable material was used through adsorbent syntheses of waste PET bottles for the removal of TC from aqueous solutions. Superior properties of nano zero valent iron and microwave energy were combined with WPET as a result of which it as concluded that 2 min MW/WPET-nZVI can be used as an alternative adsorbent for an alternative and economic environmental pollution removal method.

## Declaration of Competing Interest

None.

## Appendix A. Supplementary data

Supplementary data to this article can be found online at https://doi.org/10.1016/j.colcom.2021.100416.

## References

[1] N.A. Essawy, E.S.M. Ali, H.A. Farag, A.H. Konsowac, M. Elnoubyd, H.A. Hamade, Green synthesis of graphene from recycled PET bottle wastes for use in the adsorption of dyes in aqueous solution, Ecotoxicol. Environ. Safety 145 (57–68) (2017), https://doi.org/10.1016/j.ecoenv.2017.07.014.
[2] J.R. Jambeck, R. Geyer, C. Wilcox, T.R. Siegler, M. Perryman, A. Andrady, R. Narayan, K.L. Law, Plastic waste inputs from land into the ocean, Science 347 (2015) 768–771, https://doi.org/10.1126/science.1260352.
[3] European Strategy for Plastics, Available online. https://eur-lex.europa.eu/legal-content/EN/TXT/?uri=CELEX%3A52013DC0123 (accessed on 4 September 2020).
[4] R. Mendoza-Carrasco, E.M. Cuerda-Correa, M.F. Alexandre-Franco, C. Fernandez-Gonzalez, V. Gomez-Serrano, Preparation of high-quality activated carbon from polyethyleneterephthalate (PET) bottle waste its use in the removal of pollutants in aqueous solution, J. Environ. Manag. 181 (2016) 522–535, https://doi.org/10.1016/j.jenvman.2016.06.070.
[5] M. Elkady, H. Shokry, H. Hamad, New activated carbon from mine coal for adsorption of dye in simulated water or multiple heavy metals in real wastewater, Materials. 13 (2020) 2498, https://doi.org/10.3390/ma13112498.
[6] V.K. Gupta, T.A. Saleh, Sorption of pollutants by porous carbon, carbon nanotubes and fullerene—an overview, Environ. Sci. Pollut. Res. 20 (2013) 2828–2843, https://doi.org/10.1007/s11356-013-1524-1.
[7] S. Mousavinia, S. Hajati, M. Ghaedi, K. Dashtian, Novel nanorose-like Ce(III)-doped and undoped Cu(II)–biphenyl-4,4-dicarboxylic acid (Cu(II)–BPDCA) MOSs as visible light photocatalysts: synthesis, characterization, photodegradation of toxic dyes and optimization, Phys. Chem. Chem. Phys. 18 (2016) 11278–11287, https://doi.org/10.1039/c6cp00910g.

[8] O.L. Ungureanu, d. Bulgariu, A.M. Mocanu, L. Bulgariu, Functionalized PET waste based low-cost adsorbents for adsorptive removal of Cu(II) ions from aqueous media, Water 12 (2020) 2624, https://doi.org/10.3390/w12092624.
[9] M. Elkady, H. Shokry, A. El-Sharkawy, G. El-Subruiti, H. Hamad, New insights into the activity of green supported nanoscale zero-valent iron composites for enhanced acid blue-25 dye synergistic decolorization from aqueous medium, J. Mol. Liq. 294 (2019) 111628, https://doi.org/10.1016/j.molliq.2019.111628.
[10] R.M. Ali, M.R. Elkatory, H.A. Hamada, Highly active and stable magnetically recyclable CuFe2O4 as a heterogenous catalyst for efficient conversion of waste frying oil to biodiesel, Fuel 268 (2020) 117297, https://doi.org/10.1016/j.fuel.2020.117297.
[11] M. Elkady, H. Shokry, H. Hamad, Microwave-assisted synthesis of magnetic hydroxyapatite for removal of heavy metals from groundwater, Chem. Eng. Technol. 41 (2017) 553–556, https://doi.org/10.1002/ceat.201600631.
[12] X. Song, B. Xing, J. Feng, J. Yuana, X. Ma, X. Liua, G. Yanga, Degradation of organic dyes by persulfate using liquor grain-derived N,Pcodoped mesoporous carbon as metal-free catalyst, J. Water Process Eng. 37 (2020) 101407, https://doi.org/10.1016/j.jwpe.2020.101407.
[13] Y. Li, S. Wang, Y. Zhang, R. Han, W. Wei, Enhanced tetracycline adsorption onto hydroxyapatite by Fe(III) incorporation, J. Mol. Liq. 247 (2017) 171–181, https://doi.org/10.1016/j.molliq.2017.09.110.
[14] Z. W-Yi, R. Zhong, F.-Z. Yang, Novel fullerene-based ferrocene dyad and diferrocene triad: Synthesis and effects of introduction of fullerene[60] and phenyl linker on the thermodynamic stability, the magnetic properties and the band structure, J. Organometal. Chem 840 (2017) 75–81, https://doi.org/10.1016/j.jorganchem.2017.04.005.
[15] W.A. Khandaya, B.H. Hameeda, Zeolite-hydroxyapatite-activated oil palm ash composite for antibiotic tetracycline adsorption, Fuel. 215 (2018) 499–505, https://doi.org/10.1016/j.fuel.2017.11.068.
[16] L. Yu, W. Cao, S. Wu, C. Yanga, J. Cheng, Removal of tetracycline from aqueous solution by MOF/graphite oxide pellets: preparation, characteristic, adsorption performance and mechanism, Ecotoxicol. Environ. Saf. 164 (2018) 289–296, https://doi.org/10.1016/j.ecoenv.2018.07.110.
[17] J. Qu, Y. Liu, L. Cheng, Z. Jiang, G. Zhang, F. Deng, L. Wang, W. Han, Y. Zhang, Green synthesis of hydrophilic activated carbon supported sulfide nZVI for enhanced Pb(II) scavenging from water: Characterization, kinetics, isotherms and mechanisms, J. Hazard. Mater. 403 (2021) 123607, https://doi.org/10.1016/j.jhazmat.2020.123607.
[18] M. Hijab, P. Parthasarathy, H.R. Mackey, T. Al-Ansari, G. McKay, Minimizing adsorbent requirements using multi-stage batch adsorption for malachite green removal using microwave date-stone activated carbons, Chem. Eng. and Process. Process Intensificat. (2021) 108318, https://doi.org/10.1016/j.cep.2021.108318, in press.
[19] W. Hu, S. Cheng, H. Xia, L. Zhang, X. Jiang, Q. Zhang, Q. Chen, Waste phenolic resin derived activated carbon by microwave-assisted KOH activation and application to dye wastewater treatment, Green Process. Synth. 8 (2019) 408–415, https://doi.org/10.1515/gps-2019-0008.
[20] S.F. Adam, H. Packard, Microwave theory and applications 507, courtesy of agilent Technologies, 1969. https://uspas.fnal.gov/materials/MicrowaveTheory.pdf.
[21] E.C. Peres, J.C. Slaviero, A.M. Cunhaa, A. Hosseini–Bandegharaei, G.L. Dottoa, Microwave synthesis of silica nanoparticles and its application for methylene blue adsorption, J. Environ. Chem. Eng. 6 (2018) 649–659, https://doi.org/10.1016/j.jece.2017.12.062.
[22] L.A. Mitscher, The Chemistry of the Tetracycline Antibiotics 9, Marcel Decker Inc, N. Y, 1978, p. 330, https://doi.org/10.1002/nadc.19790270810.
[23] H. Zinnes, R.A. Comes, J. Shavel, 1, 2-benzothiazines. Iv. 1 the synthesis of 7, 8-dihydropyrido [1, 2-A][1,2] benzothiazine-10, 11 (9h, 10ah)-dione 5, 5-dioxides as 1, 2-benzothiazine analogs of partial tetracycline structures, J. Med. Chem. 2 (1967) 223–227, https://doi.org/10.1021/jm00314a020.
[24] M. Ersan, Removal of tetracycline using new biocomposite from aqueus solutions, Desalination of Water Treatment 57 (2016) (2016) 9982–9989, https://doi.org/10.1080/19443994.2015.1033765.
[25] T. Deblonde, C. Cossu-Leguille, P. Hartemann, Emerging pollutants in wastewater: A review of the literature, Int. J. Hygiene Environ. Health. 214 (2011) 442–448, https://doi.org/10.1016/j.ijheh.2011.08.002.
[26] M. Liu, L. Hou, S. Yu, B. Xi, Y. Zhao, MCM-41 impregnated with a zeolite precursor: synthesis, characterization and tetracycline antibiotics removal from aqueous solution, Chem. Eng. J. 223 (2013) 678–687, https://doi.org/10.1016/j.cej.2013.02.088.
[27] K. Choi, H. Son, S. Kim, Ionic treatment for removal of sulfonamide and tetracycline classes of antibiotic, Sci. Total Environ. 387 (2007) 247–256, https://doi.org/10.1016/j.scitotenv.2007.07.024.
[28] J. Cao, Z. Yang, W. Xiong, Y. Zhou, Y. Wu, M. Jia, S. Sun, C. Zhou, Y. Zhan, R. Zhong, Peroxymonosulfate activation of magnetic Co nanoparticles relative to an N-doped porous carbon under confinement: boosting stability and performance. 250 (2020) 117237, https://doi.org/10.1016/j.seppur.2020.117237.
[29] Q. Xu, B. Han, H. Wang, Q. Wang, W. Zhang, D. Wang, Effect of extracellular polymer substances on the tetracycline removal during coagulation process, Bioresour. Technol. 309 (2020) 123316, https://doi.org/10.1016/j.biortech.2020.123316.
[30] F. Hu, W. Luo, C. Liu, H. Dai, X. Xu, Q. Yue, L. Xu, G. Xu, Y. Jian, X. Peng, Fabrication of graphitic carbon nitride functionalized PeCoFe2O4forthe removal of tetracycline under visible light: optimization, degradation pathways and mechanism evaluation, Chemosphore. 274 (2021) 129783, https://doi.org/10.1016/j.chemosphere.2021.129783.
[31] A.M. Pandele, H. Iovu, C. Orbeci, C. Tuncel, F. Miculescu, A. Nicolescu, C. Deleanu, S.I. Voicu, Surface modified cellulose acetate membranes for the reactive retention of tetracycline, Sep. Purif. Technol. 249 (2020) 117145, https://doi.org/10.1016/j.seppur.2020.117145.
[32] X. Zhang, Y. Li, M. Wu, Y. Pang, Z. Hao, M. Hu, R. Qiu, Z. Chen, Enhanced adsorption of tetracycline by an iron and manganese oxides loaded biochar: kinetics, mechanism and column, adsorption, Bioresour. Technol. 320 (2021) 124264, https://doi.org/10.1016/j.biortech.2020.124264.
[33] J.R. Utrilla, C.V. Gómez-Pacheco, M.S. Polo, J.J. López-Peñalver, R. Ocampo-Pérez, Tetracycline removal from water by adsorption/bioadsorption on activated carbons and sludge-derived adsorbents, J. Environ. Manage. 131 (2013) 16–24, https://doi.org/10.1016/j.jenvman.2013.09.024.
[34] J. Yanga, J. Dai, L. Wang, W. Gec, A. Xie, J. He, Y. Yan, Ultrahigh adsorption of tetracycline on willow branche-derived porous carbons with tunable pore structure: isotherm, kinetics, thermodynamic and new mechanism study, J. Taiwan Inst. Chem. Eng. 96 (2019) 473–482, https://doi.org/10.1016/j.jtice.2018.12.017.
[35] V.H. Tran Thi, B. K., LeeGreat improvement on tetracycline removal using ZnO rod-activated carbon fiber composite prepared with a facile microwave method, J. Hazard. Mater. 324 (2017) 329–339, https://doi.org/10.1016/j.jhazmat.2016.10.066.
[36] U.A. Güler, Removal of tetracycline from aqueous solutions using nanoscale zero valent iron and functional pumice modified nanos cale zero valent iron, J. Envıron. Eng. Landscape Manage. 25 (2017) 223–233, https://doi.org/10.3846/16486897.2016.1210156.
[37] N.A. Elessawy, M. Elnouby, M.H. Gouda, H.A. Hamad, N.A. Taha, M. Gouda, M.S. M. Eldin, Ciprofloxacin removal using magnetic fullerene nanocomposite obtained from sustainable PET bottle wastes: Adsorption process optimization, kinetics, isotherm, regeneration and recycling studies, Chemosphere 239 (2020) 124728, https://doi.org/10.1016/j.chemosphere.2019.124728.
[38] I. Langmuir, The dissociation of hydrogen into atoms. III. The mechanism of the reaction, J. Am. Chem. 388 (1916) 1145–1156, https://doi.org/10.1021/ja02263a001.
[39] H.M.F. Freundlich, Über die adsorption in lösungen, J. Phys. Chem. 57 (1906) 385–470, https://doi.org/10.1515/zpch-1907-5723.
[40] M. Ersan, Ü.A. Güler, U. Acikel, M. Sarioglu Cebeci, Synthesis of hydroxyapatite/clay and hydroxyapatite/pumice composites for tetracycline removal from aqueous solutions, Process Saf. Environ. Prot. 96 (2015) 22–32, https://doi.org/10.1016/j.psep.2015.04.001.
[41] M. Dubinin, L.V. Radushkevich, Equation of the characteristic curve of activated charcoal, Chem. Zentralblatt. Proc. Acad. Sci. Phys. Chem. Sect. 55 (1947) 331.
[42] A. Nivaldo Módenes, G. Bazarin, C. Eduardo Borba, P. Poliane Patricia, P. Locatelli, F. Piva Borsato, V. Pagno, R. Pedrini, D. Estelita, G. Trigueros, R. Fernando, E. Quiñones, F. Bisinella Scheufele, Tetracycline adsorption by tilapia fish bone-based biochar: mass transfer assessment and fixed-bed data prediction by hybrid statistical-phenomenological modeling, J. Clean. Prod. 279 (2021) 12375, https://doi.org/10.1016/j.jclepro.2020.123775.
[43] Y. Gao, Y. Li, L. Zhang, H. Huang, J. Hu, S.M. Shah, X. Su, Adsorption and removal of tetracycline antibiotics from aqueous solution by graphene oxide, J. Colloid Interface Sci. 368 (2012) 540–546, https://doi.org/10.1016/j.jcis.2011.11.015.
[44] M. Adel, M.A.A. Mohamed, A. El-Magharaby, O. El-Shazly, E.F. El-Wahidy, Synthesis of fewlayer graphene-like nanosheets from glucose: new facile approach for graphene-like nanosheets large-scale production, J. Mater. Res. 31 (2016) 455–467, https://doi.org/10.1557/jmr.2016.25.
[45] P. Zhang, Y. Li, Y. Cao, L. Han, Characteristics of tetracycline adsorption by cow manure biochar prepared at different pyrolysis temperatures, Bioresour. Technol. 285 (2019) 121348, https://doi.org/10.1016/j.biortech.2019.121348.
[46] E.M. El-Sayed, H.A. Hamad, R.M. Ali, Journey from ceramic waste to highly efficient toxic dye adsorption from aqueous solutions via one-pot synthesis of CaSO4 rod-shape with silica, J. Mater. Res. Technol. 9 (2020) 16051–16063, https://doi.org/10.1016/j.jmrt.2020.11.037.
[47] A. Hamadi, N. Yeddou-Mezenner, A. Lounis, R.M. Ali, R.H. Hamad, Upgrading of agro-industrial green biomass residues from chocolate industry for adsorption process: diffusion and mechanistic insights, Food Sci. Technol. 58 (2021) 1081–1092, https://doi.org/10.1007/s13197-020-04622-z.
[48] J. Cao, Z. Xiong, B. Lai, Effect of initial pH on the tetracycline (TC) removal by zero-valent iron: adsorption, oxidation and reduction, Chem. Eng. J. 343 (2018) 492–499, https://doi.org/10.1016/j.cej.2018.03.036.